Microbial Adhesion in Flow Displacement Systems

Henk J. Busscher and Henny C. van der Mei*

*Department of Biomedical Engineering, University Medical Center Groningen and
University of Groningen, 9700 AD Groningen, The Netherlands*

INTRODUCTION

Microbial adhesion to surfaces is the onset of the development of a biofilm. Biofilm formation occurs on all surfaces exposed to an aqueous environment, such as soft tissues, implanted biomaterials or tooth surfaces in the human body, rocks in rivers, pipelines in water works, and on ship hulls (51). Generally, microbial adhesion is preceded by the formation of a conditioning film of macromolecular components (3, 80), after which mass transport processes ensure initial adhesion of microorganisms. However, clinically, microbial adhesion to surgical instruments, light switches in the operating theater and cotton fabrics in the absence of a conditioning film may also add to the transmission of pathogens in a hospital environment. Initial adhesion is reversible for a short period of time (59, 90), after which adhering organisms start to anchor themselves irreversibly through extracellular polymeric substance production (25, 63). Coadhesion phenomena may start (6, 71) and finally the organisms commence to grow, with a mature biofilm as a result.

The rate of adhesion is determined by the number of microorganisms transported to a substratum surface through mass transport processes such as convection, diffusion, or sedimentation (40, 51, 95). In relatively stagnant environments, such as the oral cavity or at implanted biomaterial surfaces, convective mass transport, i.e., transport through liquid flow of suspended organisms, only plays a minor role and sedimentation and diffusion are the main means of mass transport. However, on ship hulls, in rivers, or in water works, convective mass transport of suspended microorganisms is the major mechanism that controls the rate of microbial adhesion.

Usually, increased fluid flow towards or parallel to a substratum surface results in faster adhesion of microorganisms due to higher mass transport (82), despite the presence of

* Corresponding author. Mailing address: Department of Biomedical Engineering, University Medical Center Groningen and University of Groningen, P.O. Box 196, 9700 AD Groningen, The Netherlands. Phone: (31) 503633140. Fax: (31) 503633159. E-mail: h.c.van.der.mei @med.umcg.nl.

higher fluid shear stimulating their detachment (14). However, when fluid flow exceeds a critical limit (49), resulting wall shear rates may become high enough to prevent adhesion (65, 78) or even stimulate detachment. For instance, in aqueous suspensions, wall shear rates of 6,000 to 8,000 s^{-1} (equivalent to shear forces of between 6×10^{-3} and 8×10^{-3} nN) were sufficient to prevent adhesion of *Pseudomonas fluorescens* to stainless steel, while wall shear rates of 12,000 s^{-1} (or shear forces of 12 $\times 10^{-3}$ nN) could detach adhering organisms (78). Adhesion of *Staphylococcus aureus* to collagen-coated glass plates increased for shear rates between 50 and 300 s^{-1} due to increased mass transport and then, after exceeding the critical limit, decreased for shear rates higher than 500 s^{-1}, equivalent to a shear force of 0.5×10^{-3} nN (64). Note the enormous range in adhesive forces between different strains and species. Similar forces were derived from a centrifugal force assay assessing perpendicular detachment forces (74) for *Streptococcus sanguis* (0.2×10^{-3} nN) and *Actinomyces viscosus* (1.1×10^{-3} nN). Furthermore, turbulent flow as opposed to a laminar regimen is known to affect biofilm architecture (72, 85, 100, 102). Biofilms grown under turbulent flow tend to form filamentous streamers, while those grown under laminar flow have a more uniform cell distribution. Turbulent flow also creates more stable and rigid biofilms than laminar flow.

The implications of studies on initial microbial adhesion and detachment reach beyond the stage of initial adhesion and have great relevance for the maintenance of a biofilm on a surface. A biofilm is usually modeled as a dense, base biofilm, combined with a more open-structured surface biofilm (103), but a complete biofilm model should, in our opinion, include the role that the initially adhering organisms play in linking a biofilm to a substratum surface (7). Organisms in the linking film are those that initially adhered to the substratum surface and whose retention is crucial for the maintenance of the entire biofilm on a surface and during periods of high shear-off forces. Organisms residing in the linking film are therefore under direct control of the substratum surface. Linking film organisms adhere to almost any substratum, regardless of its surface properties, but are not always able to maintain their position under environmentally or medically relevant shear conditions (12). In this respect, we have suggested in the past that more studies should aim towards "bacterial retention" rather than to "bacterial adhesion" (31).

Adhesion of microorganisms to substratum surfaces and their retention are difficult to measure (2) apart from the fact that a proper distinction between both definitions is seldom made, and a variety of static and dynamic flow displacement systems has been developed by different research groups, currently often with the aid of image analysis (58, 70, 87, 97, 106). Dependent on the microscopic technique used, adhering microorganisms both on transparent substrata on metals (94) and dental enamel surfaces (45, 71, 93) can be visualized. Sometimes mass transport considerations are included in the experimental design, but frequently no distinction is made between kinetic and stationary or equilibrium effects. Especially in systems that are stirred or shaken to prevent sedimentation, mass transport to substratum surfaces is often limited because the organisms are carried around by the flow rather than toward a substratum surface. The lack of a ubiquitously accepted methodology and way of reporting bacterial adhesion data impedes a comparison of results from different laboratories and is unlike the standardization seen in many other fields of science.

Contributing to this unfortunate situation are the so-called "slight-rinsing" and "dipping" artifacts to remove loosely adhering bacteria. In a typical Materials and Methods section of a paper on bacterial adhesion it can be read that "substrata with adhering bacteria were slightly rinsed under running tap water" or "dipped to remove loosely adhering bacteria prior to enumeration" (for recent examples see references 18, 29, 55, and 88). Such methodology has been (and still is in many research groups) general practice for many years, but nevertheless is inadequate as it raises a number of obvious questions: (i) what is the magnitude of the rinsing forces applied, (ii) what is the definition of "loosely adhering" bacteria, i.e., at what rinsing forces are they detached, and (iii) what percentage of the total adhering population is removed by rinsing?

To avoid these questions, we have started doing microbial adhesion experiments in a parallel plate flow chamber under controlled hydrodynamic conditions (83). Flawed experimental procedures involving "slight rinsing" and "dipping" artifacts neglect observations over the past decades that a passing air-liquid interface has the ability to displace and detach micronsized particles, including dust particles (47) and adhering microorganisms (30, 73), from surfaces. By consequence, upon close inspection many papers on microbial adhesion do not deal with adhesion, but with the ability of adhering organisms to withstand detachment, i.e., microbial retention. Bos et al. (7) demonstrated, using micropatterned surfaces, that bacterial adhesion is less influenced by substratum surface hydrophobicity than bacterial retention.

In fact, in many natural processes bacterial retention has been described to be more influential on the final development of a biofilm than adhesion. In the oral cavity, for instance, adhering bacteria have to withstand detachment forces due to eating, speaking, drinking and swallowing in order to form a biofilm. On the eye and on contact lenses, blinking of the eyelid creates a detachment force on adhering bacteria (38), similar to the action of waves on rocks and ship hulls in the marine environment. Adhering organisms, responsible for biodeterioration of monumental buildings (42), have to adhere strongly enough to withstand rain. In this respect it is interesting that freshwater, multispecies biofilms at solid-liquid interfaces occur both in quiescent waters and in conditions of high shear. In the latter case, however, increases in shear rate decreased the microbial diversity in the biofilm (77), likely because weakly adhering strains could not maintain their position in the biofilm under high shear forces. Either increasing shear rates may present a challenge to the linking organisms in a biofilm, possibly leading to detachment at the interface between the biofilm and a substratum surface, or if this link appears stronger than the cohesive forces holding the biofilm together, increased shear rates may make the biofilm thinner. Chang et al. (13) reported for water biofilms that this thinning coincided with the biofilm becoming denser.

In summary, there are three principal reasons to use flow displacement systems in microbial adhesion research.
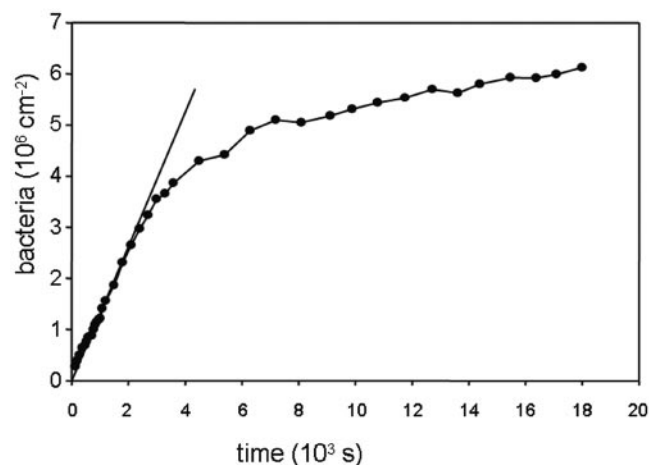
FIG. 1. Example of deposition kinetics as a function of time in a parallel plate flow chamber, reaching a (pseudo-) end stage for *Enterococcus faecalis* OG1X on fluoroethylenepropylene in phosphate-buffered saline, pH 7.0, at a concentration of 3×10^8 bacteria per ml and a wall shear rate of 10 s^{-1}. The tangent shows the linear trajectory from which the initial deposition rate is calculated.

FIG. 3. Area blocked by an adhering organism can be obtained from radial distribution function and other organisms arriving at a substratum surface cannot adhere in this area. Note that the blocked area can depend on fluid flow: top, slow fluid flow; bottom, fast fluid flow.

Mass Transport

For a proper analysis of adhesion data, kinetic and stationary or equilibrium effects must be distinguished. Typical kinetics of any bacterial adhesion experiment follows a pattern as shown in Fig. 1, where an initial linear trajectory can be seen, followed by a leveling off to a (pseudo-) end stage. During the initial phase, organisms that arrive at a substratum surface interact solely with the substratum surface, and the rate at which organisms adhere in this stage of an experiment can be considered as representative for the true affinity of an organism for a given substratum surface (Fig. 2). At later stages, when a substratum surface is already partially covered with adhering organisms, an arriving organism will have interaction with the substratum surface, but also with already adhering microorganisms (Fig. 2) and thus the data will reflect contributions from different interactions that are hard to separate. Typically, the kinetics level off due to blocking (Fig. 3) of available substratum surface by adhering microorganisms yielding an end stage.

A pseudo-end stage can be reached, however, when a microbial suspension is depleted of organisms due to their adhesion to the substratum, while mass transport in the system used

is inadequate to replenish and restore a high concentration near the substratum surface (Fig. 4). Flow displacement systems allow control of mass transport and theoretical calculation of the (maximum) mass transport that can be expected on the basis of flow velocities, microbial concentrations in suspension and dimensions of the flow system (22).

The end stage of an adhesion experiment is said to be stationary if reversibility is absent or cannot be proven. In an equilibrium stage, adhesion is reversible and desorption and adsorption events balance each other. While stationary end stages are reached faster at higher microbial concentrations in suspension, the end stage is usually not affected. For an equilibrium end stage, however, end stage adhesion increases with the microbial concentration in suspension (Fig. 5). Although initial microbial adhesion is generally said to be reversible, this is only so during the first minutes of contact between an organism and a surface and bond aging rapidly yields a virtually irreversible stage, as observed directly in flow displacement systems (60) and recently confirmed by direct force measurements between bacteria and substratum surfaces as a function of time, applying atomic force microscopy (AFM) (90). This type of bond aging should not be confused by the transition to more irreversible binding of adhering bacteria by extracellular polymeric substance production, which is a metabolic process contributing to irreversible adhesion. All colloidal particles, including microorganisms, exhibit bond aging, often toward a more irreversible state, by the slow removal of interstitial water facilitating closer approach or reorientation of interacting sites.
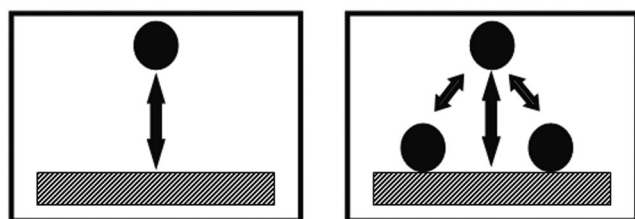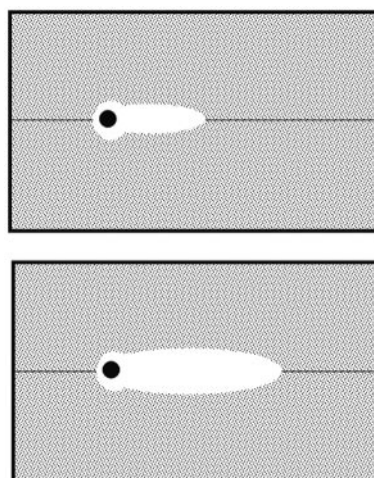

FIG. 2. An organism arriving at a substratum surface in the initial phases of adhesion interacts solely with the substratum surface (left), while at later stages interaction is with the substratum surface as well as with already adhering organisms (right).

Wall Shear Rates

The use of flow displacement systems allows calculating the wall shear rate (s^{-1}) acting on adhering microorganisms, as the main source of fluid flow forces on adhering organisms. At a surface, fluid flow is essentially absent and flow increases with distance away from the surface. Consequently, fluid flow is slightly higher over the top of an adhering microorganism than
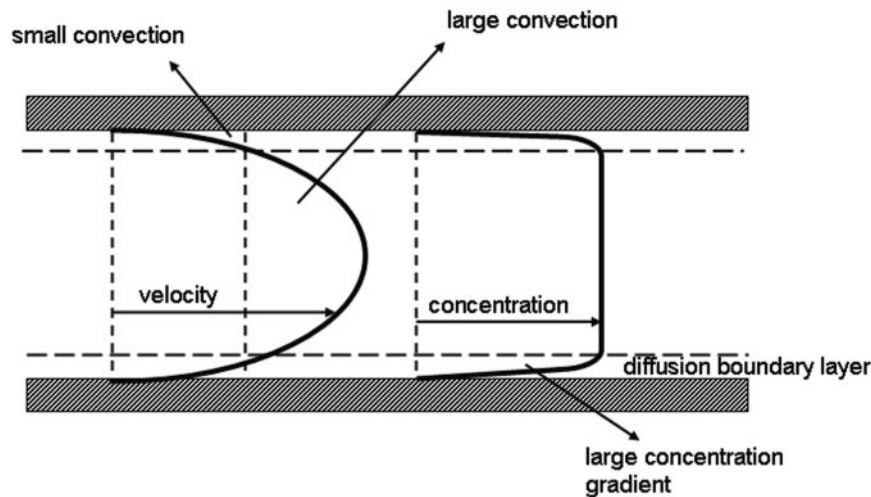
FIG. 4. Velocity and bacterial concentration as a function of depth in a parallel plate flow chamber. Convection and diffusion contribute to the maintenance of a high microbial concentration near a substratum surface in flow displacement systems, whereas in stagnant systems mass transport solely relies on diffusion. Convection in a flow displacement system contributes to the development of a stable concentration despite bacterial removal from the suspension through adhesion.

at its bottom, which yields a shear. The force resulting from this shear acts parallel to the surface and depends on the viscosity of the suspension and the microbial dimensions. At this point, it is important to emphasize that the adhesion forces arising from a perfectly smooth and homogeneous substratum

FIG. 5. Examples of the influence of concentration on the kinetics of microbial adhesion for equilibrium (top) and stationary endpoint (bottom) adhesion. Equilibrium endpoint adhesion increases with bacterial concentration in suspension, whereas for stationary endpoint adhesion the endpoint is reached faster only upon a concentration increase.

surface act perpendicular to the surface (6, 23). This implies that under ideal conditions shear cannot cause detachment, but only sliding (lateral movement of adhering bacteria on a surface) of an adhering organism until it encounters less favorable conditions on a surface and detaches. Whether sliding occurs under the influence of shear depends on immobilization forces, which must have a component parallel to the surface and may arise from local heterogeneities or rugosities.

The wall shear rate that develops in a system depends not only on the fluid flow rate (ml s^{-1}) or fluid velocity (m s^{-1}), but also on the dimensions of the system. This point is often overlooked in the literature, and many papers in which flow displacement systems are employed report flow rates or fluid velocities, leaving it to the reader to express results in terms of wall shear rates, necessary for a comparison with other experimental systems and environmental conditions (Table 1). The simple realization that a flow in a riverbed leads to a different wall shear rate than the same flow in a narrow pipe or tubing illustrates the importance of reporting wall shear rates instead of only flow rates, most certainly when the latter are given in the absence of the dimensions of the flow chamber.

TABLE 1. Summary of environmental shear rates, as taken from the literature

Phenomenon	Shear rate (s^{-1})	Reference
Channels within a biofilm	60–300	86
Blinking of the eye	0.35	38
Bile drain	10	101
Oral cavity due to salivary flow	0.1–50	8
Oral cavity while biting an apple	200	28
Urinary catheter	15	98
Ship in harbor	50	1
Ship navigating (turbulent flow)	125,000	1
Flow of a film over a vertical plate	0.1	8
Tumbling or pouring	10–100	8
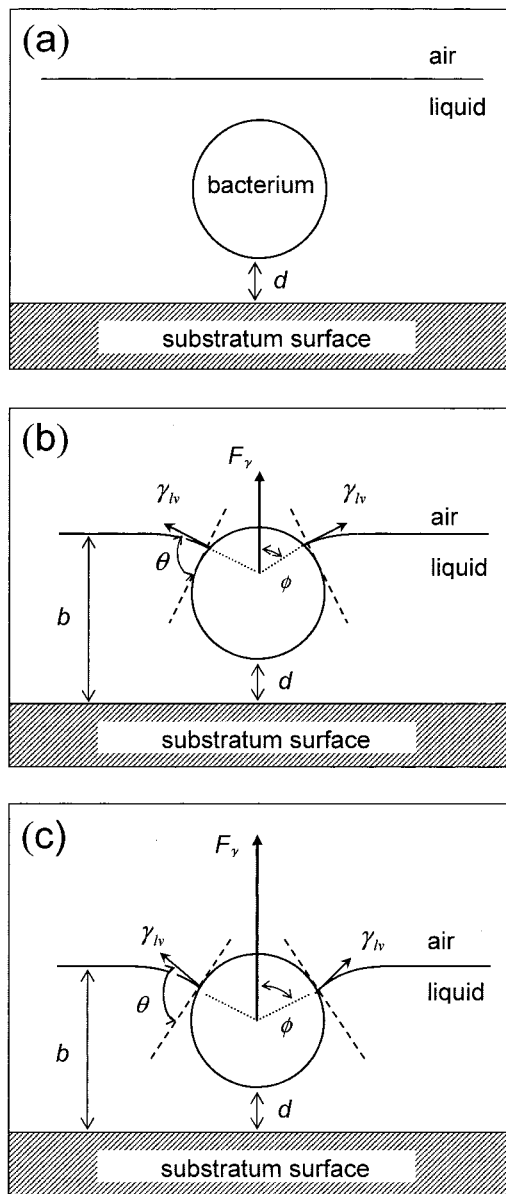
FIG. 6. Schematic presentation of the different degrees of immersion of a bacterium upon the passage of an air bubble. The air-liquid interface velocity decreased from panel a to panel c, yielding to different degrees of immersion. d represents the distance between the bacterium and the substratum surface, ϕ is the angle giving the position of the particle with respect to the air-liquid interface, θ is the contact angle between the surface of the bacterium and the air-liquid interface, b is the liquid film thickness, γ_{lv} is the air-liquid interfacial tension, and F_γ is the surface tension result of the air-liquid interfacial tension exerted by the bend meniscus on the bacterium. (Reprinted from reference 30.)

Artifacts

Artifacts are most easily created in microbial adhesion experiments, of which the "slight rinsing" and "dipping" artifacts are the most notorious. The same surface tension forces that allow small insects to walk on water can lift adhering microorganisms from a substratum when they intercept an adhering

organism (Fig. 6). Opposite to wall shear forces, these surface tension detachment forces work perpendicular to a substratum surface and thus directly oppose the adhesion forces. Moreover, the surface tension detachment forces can be in excess of the adhesion forces by several orders of magnitude and cause sizeable detachment of adhering microorganisms from surfaces. Unfortunately, this detachment is dependent on the microbial strain involved and whereas some strains and species adhere strongly enough to withstand these detachment forces, others show complete detachment upon one passage of a liquid-air interface over a substratum surface (12, 30). In short, these forces are not controlled in many experimental systems and bear no realistic relationship to those experienced in natural systems.

The aim of this review is to present a comprehensive guideline to microbiologists interested in studying microbial adhesion to surfaces with the aid of flow displacement systems, focusing on laminar flow in spatially confined systems. First, essentials of hydrodynamics will be briefly discussed, followed by strategies for data analysis and design aspects of flow displacement systems, including observation methodologies, as well as their limitations. This of course does not complete a full description of the proper use of flow displacement systems, and especially the choice of organisms, whether fresh clinical isolates or strains taken from a culture collection are used, is influential on the final results (2), because strains tend to lose their adhesive properties when kept in stock (46). However, this issue is considered outside the scope of this review. This review is concluded with selected examples, highlighting the benefits of flow displacement systems.

ESSENTIALS OF HYDRODYNAMICS

Basic Equations for Fluid Flow in Model Systems

Flow rates and velocities. There are two commonly used configurations of flow displacement systems by which most situations occurring in clinical practice can be assessed. These include flow through a cylindrical pipe or tubing as a model for, e.g., urinary catheters, vascular catheters, bile drains, stents, etc., and flow through a rectangular channel or between two parallel plates, as for instance the surface of a voice prosthesis versus the esophageal wall.

The (volumetric) flow rate, usually indicated as Q and expressed preferably in $m^3 s^{-1}$ or sometimes for practical reasons in ml min^{-1} or ml s^{-1}, describes the volume of fluid passing through the system, regardless of its dimensions. The resulting average velocity of the flow, v_{av} (m s^{-1}), on the other hand, is greatly dependent on the cross-sectional area of the flow system and can be simply obtained by dividing the flow rate by the cross section, which equals $\pi \times r^2$ for a pipe or tubing with radius r or $w_0 \times h_0$ for a rectangular channel of width w_0 and height h_0.

The velocity of the flow, however, is different at different distances from the walls of a flow system and increases parabolically toward the center according to Poiseuille's law. At the wall, the flow velocity is zero.

Wall shear rates and other hydrodynamic forces. The main hydrodynamic force exerted by the flow on an adhering organism is determined by the velocity gradient near the wall. This

TABLE 2. Simple equations for wall shear rates, Reynolds and Péclet numbers, and approximated SL solutions for convective-diffusion
at a distance x from the flow system inlet, valid for cylindrical and rectangular flow displacement systems

Configuration of the flow	Wall shear rate	Reynolds number	Péclet number	SL initial deposition rates
Cylindrical	$\dfrac{3Q}{\pi r^3}$	$\dfrac{Q\rho}{\pi r\eta}$	$\dfrac{3v_{av}R_b^{3}}{r^2 D_\infty}$	$0.678\dfrac{D_\infty c_b}{R_b}\left(\dfrac{Pe\cdot r}{x}\right)^{1/3}$
Rectangular	$\dfrac{3Q}{2(h_0/2)^2 w_0}$	$\dfrac{\rho Q}{(w_0+h_0)\eta}$	$\dfrac{3v_{av}R_b^{3}}{2(h_0/2)^2 D_\infty}$	$0.538\dfrac{D_\infty c_b}{R_b}\left(\dfrac{Pe\cdot h_0}{x}\right)^{1/3}$

force is proportional to the increase in fluid velocity from the surface (where fluid velocity is zero), which is known as the wall shear rate σ (s^{-1}). Wall shear rates can be calculated from velocity profiles determined with either particle image velocimetry (79) or numerical simulation (3) using

$$\sigma = (dv/dh) \qquad (1)$$

where v is the velocity in the direction of the main flow and h (meters) is distance directed perpendicular to the substratum surface in a flow chamber. For laminar flow in cylindrical and rectangular displacement systems, wall shear rates can be calculated by the equations listed in Table 2 (22). A summary of the terms used in the equations discussed in this article appears in Table 3.

The hydrodynamic force per unit surface area exposed to a flow as a result of wall shear rate is directed parallel to the wall and is defined as the shear stress τ_w ($N\ m^{-2}$), which follows

from multiplying the shear rate with the absolute viscosity η ($kg\ m^{-1}\ s^{-1}$) of the fluid involved (53):

$$\tau_w = \eta\sigma \qquad (2)$$

Multiplication of the shear stress by the area of the adhering organism as exposed to the flow directly yields the shear force (N) acting on the organism. As, in principle, shear forces operate at a 90-degree angle of the adhesive forces, acting perpendicular to a substratum surface, shear can only cause detachment due to rolling phenomena in combination with minor surface roughness and chemical heterogeneities. Indeed, bacterial detachments under such conditions have been observed (78). Lift forces due to fluid flow do act perpendicularly to a surface, but are generally considered too weak to cause microbial detachment.

Dimensionless numbers: Reynolds and Péclet. In hydrodynamics, dimensionless numbers are often used to describe certain properties of a system. These numbers are made dimensionless, so that the properties to be derived from these numbers are not influenced by system dimensions, such as width, height, etc., or flow rate. The Reynolds number is an important number, as it describes when flow changes from laminar to turbulent. Most equations given in this paper deal with a laminar flow, that is, Reynolds numbers less than 2,000. Table 2 summarizes the equations needed to assess the Reynolds number for different configurations. Table 2 also summarizes the equations needed to calculate the so-called Péclet number. The Péclet number defines the ratio of convective over diffusional mass transport in a flow displacement system.

TABLE 3. Nomenclature with preferred units

A_b, blocked area (m^2)
D_∞, diffusion coefficient, around 10^{-13} for microorganisms ($m^2\ s^{-1}$)
E, efficiency of air bubble detachment
Le, development of steady laminar flow (m)
Pe, Péclet number
Q, volumetric flow rate ($m^3\ s^{-1}$)
R_B, microbial radius (m)
Re, Reynolds number
$g(r)$, radial distribution function
h_0, height of a rectangular channel (m)
j_0, initial deposition rate ($cm^{-2}\ s^{-1}$)
$n(t)$, number of organisms adhering at time t (m^{-2})
n_∞, number of organisms adhering at time ∞ (m^{-2})
r, radius of a cylindrical channel (m)
t, time (s)
t_d to t_a, residence time of an adhering organism (s)
v_{av}, average flow velocity ($m\ s^{-1}$)
w_0, width of a rectangular channel (m)
x, distance along the flow from the inlet (m)
α, deposition efficiency
β, desorption rate coefficient (s^{-1})
$1/\delta$, characteristic time for bond aging (s)
γ_{1v}, liquid surface tension ($mJ\ m^{-2}$)
η, absolute viscosity ($kg\ m^{-1}\ s^{-1}$) ($10^{-3}\ kg\ m^{-1}\ s^{-1}$ for aqueous solutions)
ϕ, angle determining the position of an organism with respect to an air-liquid interface (degrees)
θ, contact angle between the surface of a microorganism and an air-liquid interface (degrees)
ρ, fluid density ($kg\ m^{-3}$)
σ, wall shear rate (s^{-1})
τ, characteristic deposition time constant (s)
τ_w, wall shear stress ($N\ m^{-2}$)

Mass Transport Considerations

Convective-diffusion equation. Microbial deposition from flowing suspensions onto substratum surfaces depends critically on mass transport processes. In fully stagnant systems, mass transport is slow, because microbial transport is solely due to diffusion. Typical values for microbial diffusion coefficient range from $2.9 \times 10^{-13}\ m^2\ s^{-1}$ to $5.0 \times 10^{-13}\ m^2\ s^{-1}$ (92, 107), indicating that diffusional transport over a length equal to the dimensions of an organism takes approximately 2 to 3 s. In flow displacement systems, mass transport is always a combination of convection and diffusion. Since the fluid film adjacent to a substratum surface is essentially stagnant too, crossing this diffusion boundary layer of typical thickness of $0.06 \times 10^{-4}\ m$ (92) requires about 7 s regardless of fluid flow. Convective fluid flow, however, is necessary to maintain a high enough concentration near the substratum surface to ensure favorable conditions for diffusion. Consequently, mass transport in flow displacement systems is through a combi-

nation of convection and diffusion (Fig. 4).

Sedimentation may contribute to mass transport as well, both in a negative as well as in a positive sense, depending on the configuration of the system. Sjollema et al. (82) in the past have eliminated the contribution of sedimentation to mass transport in a parallel plate flow chamber by arguing that sedimentation negatively contributed to deposition to the top plate of the chamber and positively to the bottom plate (provided horizontal positioning of the chamber), yielding the conclusion that by averaging the deposition rates on the top and bottom plates a sedimentation-less deposition rate could be obtained. Depending on the strain employed, deposition rates for the top and bottom plates could differ by a factor of 7.

Mathematically, theoretical mass transport in a given flow displacement system can be calculated by solving the so-called convective-diffusion equation, which is an extremely complicated mathematical procedure considered outside the scope of this review and for which we refer the reader to reference 22.

Approximate solutions for current flow displacement systems. Fortunately, approximate solutions such as the Smoluchowski-Levich (SL) approximation exist for determining mass transport in flow displacement systems (22). In the SL approximation it is assumed that the substratum surface acts as a perfect sink, i.e., all microorganisms sufficiently close to the surface adhere irreversibly. In general, however, experimentally observed deposition rates are much smaller than predicted by the SL approximation (56) unless the repulsive electrostatic interactions between the collector surfaces and the depositing organisms are reduced by increasing the ionic strength of the suspending fluid.

In the Smoluchowski-Levich solution, the attractive interactions between microorganisms and a substratum surface are assumed to be counterbalanced by increased viscous forces near the surface. These assumptions in practice mean that the SL solution for mass transport in flow displacement systems must be considered as an upper limit for the mass transport possible in a given configuration. Calculation of this upper limit is strongly advised, as it yields a reference number for the initial deposition rates experimentally observed, whereas otherwise data would just present a meaningless number. Moreover, the ratio between the experimentally observed microbial deposition rates and the SL deposition rates indicates the fraction of all arrivals of organisms at a substratum surface that actually adhere, for which the term deposition efficiency α has been reserved. Sjollema et al. (82), for instance, noted that the deposition efficiency of oral streptococci in a parallel plate flow chamber amounted to only 20 to 30% of the theoretical upper limit given by the SL approximate solution when accounting for sedimentation (Table 2 summarizes the SL upper limits for mass transport in different flow displacement systems). For polystyrene particles, however, with similar surface hydrophobicity and charge, the deposition efficiency was only 5%, from which it was concluded that fibrillar surface appendages contribute to mass transport in a way not accounted for in the SL approach.

Coagulase-negative staphylococci with little or no surface charge could deposit on negatively charged biomaterials with deposition efficiency higher than unity (1.4 to 1.9), likely because their radius, including the length of possible protruding surface appendages, as necessary in the SL approach could not be reliably assessed. Due to this phenomenon, their deposition efficiencies to positively charged surfaces were found to be as high as 2.4 (91).

Liquid-Air Interface

Detachment of an adhering microorganism from substratum surfaces by a passing liquid-air interface or air bubble during slight rinsing or dipping, as discussed above, is controlled by a sequence of processes that includes the approach of the air bubble to an adhering microorganism, interception of the organism by the air bubble, deformation of the air-liquid interface, yielding a thin liquid film separating the organism and air bubble, formation of a three-phase contact between an adhering organism, air and liquid, and subsequent transport of the bacterium-bubble aggregate away from the substratum surface (30). Hence, the efficiency of microbial detachment (E) by a passing air-liquid interface can be expressed as (35)

$$E = E_C \times E_A \times E_S \qquad (3)$$

in which E_C is the air bubble-organism collision efficiency, E_A is the bubble-organism attachment efficiency, and E_S denotes the stability of the bubble-organism aggregate.

The direction and velocity of the air bubble with respect to the adhering microorganism determine the collision efficiency (E_C) (68). In a rectangular or cylindrical flow chamber, for an air bubble fully spanning the width of the chamber, the collision efficiency is one. However, an air bubble moving in a narrow channel is surrounded by a liquid film (10), the thickness of which increases with increasing air bubble velocity. As this liquid film thickness decreases, the collision efficiency increases, as outlined in Fig. 6.

The interaction between a passing air bubble and an adhering microorganism in an aqueous medium includes, apart from hydrodynamic forces, Lifshitz-Van der Waals, electrostatic, and hydrophobic (acid-base) forces (35). Hence, the bubble-organism attachment efficiency (E_A) will increase with cell surface hydrophobicity (24). Note that an effective three-phase contact between the bubble and an adhering organism (Fig. 6) can only form when the bubble contact time is long enough to thin the liquid film and form a three-phase boundary (36). Hence, the bubble attachment efficiency (E_A) will also increase with decreasing air bubble velocity. During thinning of the liquid film, a viscous force opposes the attachment of the microorganism to the air bubble. This viscous drag force increases with the size of the organism and the air bubble velocity (30).

Once and only if an effective three-phase contact between the bubble and an adhering organism has formed, a balance between the surface tension force, F_γ, the bacterial adhesion force, F_A, and the viscous drag force, F_η, determines whether detachment will occur. Evidently (Fig. 6), the surface tension force opposes the adhesion and viscous drag forces depending on the position of the three-phase contact and can be expressed by

$$F_\gamma = 2\pi R_B \gamma_{1v} \sin[\phi(t)] \sin[\theta - \phi(t)] \qquad (4)$$

in which R_B is the radius of the bacterium, ϕ represents the angle determining the position of the bacterium with respect to the air-liquid interface and θ is the contact angle between the
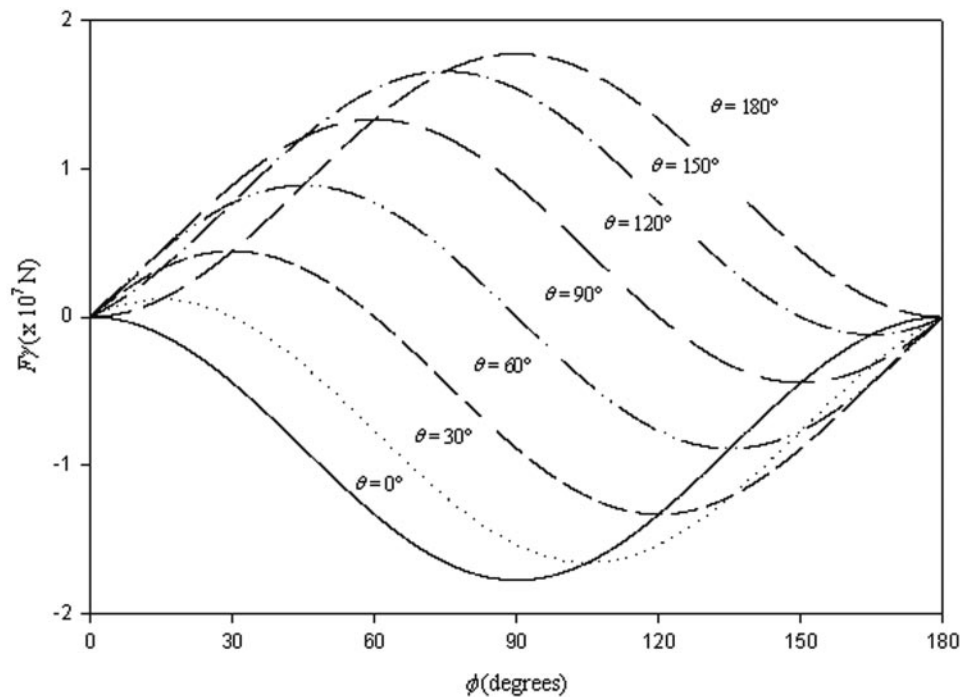
FIG. 7. Theoretically calculated surface tension detachment forces from $F_\gamma = 2\pi R_B \gamma_{1v} \sin[\phi(t)] \sin[\theta - \phi(t)]$ for different values of ϕ and θ, for a bacterium of radius R_B 800 nm and γ_{1v} 72 mJ m^{-2}. Positive forces are directed away from the substratum surface. (Reprinted from reference 30.)

surface of the bacterium and the air-liquid interface (other symbols follow from Fig. 6). Figure 7 presents the surface tension detachment force as a function of ϕ for different microbial contact angles or cell surface hydrophobicities, θ. As can be seen, for each cell surface hydrophobicity, the surface tension detachment force passes through a maximum value at a different degree of immersion of the adhering organisms (compare Fig. 6).

Recent estimates of bacterial adhesion forces have become available from atomic force microscopy and range from 7 to 4 nN between sulfate reducing bacteria and Si_3N_4 or mica surfaces (23). Such adhesion forces are orders of magnitude larger than derived from hydrodynamic and centrifugal force measurements, but much smaller than the surface tension detachment forces induced by a passing air-liquid interface, ranging up to 200 nN, as can be seen in Fig. 7. It is likely, however, that each experimental technique measures a different type of interaction force. The tip of an atomic force microscope is forced through the entire cell surface until it hits the cell wall and thus has ample opportunity to establish contact sites. In macroscopic adhesion, contact sites may be confined to outer cell surface sites, while also the contact area may be larger than when an atomic force microscope tip is applied. Reliable measurement and interpretation of microbial interaction forces must thus be considered as a field still open for research.

Once detached from a substratum surface, the balance between the surface tension forces acting on the microorganisms as opposed to external forces in the flow (i.e., gravitational force, buoyancy force, hydrostatic pressure and viscous drag force opposing the separation of the organisms from the collector surfaces) determines the aggregate stability (E_S) (81).

DESIGN ASPECTS OF FLOW DISPLACEMENT SYSTEMS

Ideally, the design of a flow displacement system should allow ample opportunity for the fluid flow to develop a steady, laminar profile according to Poiseuille's law. By analyzing the velocity profile under relevant shear rates at different positions in the system (Fig. 8) this can be checked and usually higher shear rates set more stringent requirements to the design of a system.

The area of a parallel plate flow chamber where a constant velocity profile is present for a range of shear rates represents the quality of that flow chamber. Alternatively, in a stagnation point flow chamber, fluid flow changes from essentially stagnant in the center of a substratum surface and then increases radially outward. This enables us to study microbial deposition under various shear conditions in one and the same experiment, although the use of a stagnation point flow chamber requires transparency of the substrata under study, opposite to the parallel plate flow chamber. The parallel plate flow chamber offers more versatility with respect to the choice of substrata and in addition is conceptually much simpler than the
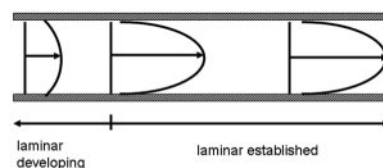

FIG. 8. Development of an established parabolic flow between parallel plates.
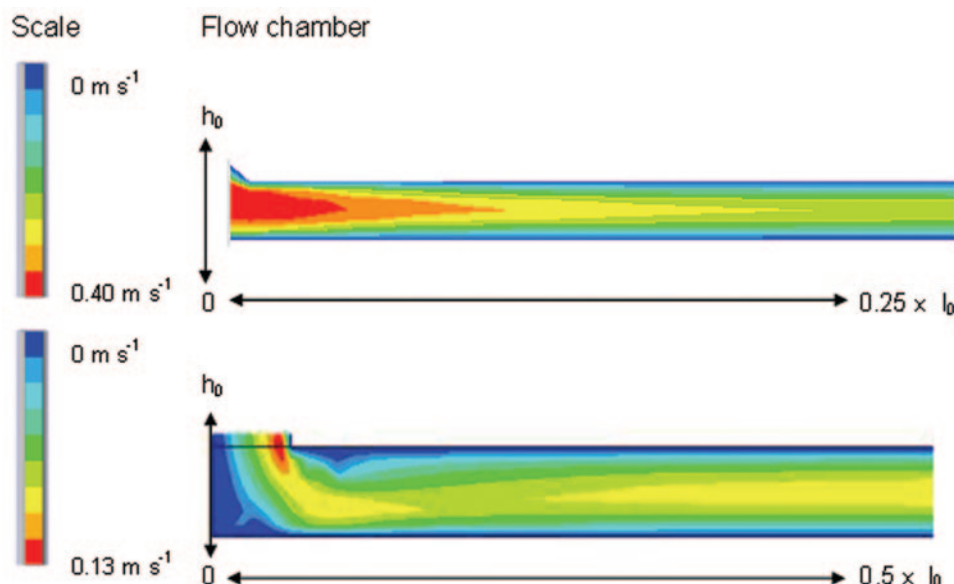
FIG. 9. Modeled velocity profiles in longitudinal cross section from the inlet to the center of parallel plate flow chambers. Top chamber A shows a well-developing profile that has become established within 25% of the length of the chamber (no more changes in color or color widths), whereas the bottom chamber B continues to develop over more than half the length of the chamber. Scale colors indicate flow velocities. (Reprinted from reference 4.)

stagnation point flow chamber. Therefore, the parallel plate flow chamber will be used in the next sections to illustrate the importance of design features of a flow displacement system. In this section too, attention will be paid to observation methodologies and data analysis strategies.

Development Length and Design Aspects in the Parallel Plate Flow Chamber

In the design of a flow chamber, concessions have to be made quite frequently due to limitations in size, construction material, reuse and flexibility of the substratum, and eventually the costs of construction. Yet the design appears crucial if a flow chamber is to be applicable over a wide range of flow rates. Several designs currently used (4) are flawed in the design of the inlet and outlet, because only a minor fraction of the bottom plates could be used for adhesion studies, and then again, only over a limited flow range. To indicate the importance of the inlet design, Fig. 9 compares the flow in the inlet of two parallel plate flow chambers. The gradual transition in a parallel plate flow chamber A (Fig. 9, top) results in an area with high fluid velocity, which remains located at the same position for high and low flow rates, without affecting the establishment of flow in the observation area. At low flow rate in differently designed parallel plate flow chamber B (Fig. 9, bottom), which is characterized by an inlet with two sharp bends, a Poiseuille flow already develops close to the inlet, whereas at a slightly higher flow rate a clearly disturbed flow enters the chamber, indicated by changing fluid velocities in the length direction (the irregular color distribution).

Although parallel plate flow chamber A has the inlet and outlet positioned under an angle, it still allows the largest range in shear rates to be used, due to the length of the channel. The design highly affects the region for uniform flow and subsequently ob-

servation of microbial adhesion. In combination with the length available for establishment of flow, the inlet geometry determines whether a flow chamber can be used as a valid model to study bacterial adhesion for the problem under investigation.

Some simple calculations allow determining the length required for the desired flow to develop. For a rectangular cross section (9, 96) the distance Le required for the establishment of a steady, laminar flow is calculated as follows.

$$Le = \text{constant} \times h_0 \times Re \qquad (5)$$

Values for the proportionality constant range from 0.013 (96) to 0.044 (9), the latter constituting a more stringent criterion. Based on the Bowen criterion, for a flow displacement system with inlet and outlet in the direction of the flow and allowing 2.5-cm establishment length, Re numbers up to 1,000 can be applied. For most dimensions of flow chambers published in the literature this coincides with shear rates well over 10,000 s^{-1}, covering the clinically relevant range of shear rates (Table 1). In other words, the ideal flow chamber is as long as practically possible and should avoid changes in the direction of flow, i.e., the directions of the inlet and outlet should be in the direction of flow through the chamber.

Observation Methodologies

For observation of adhering microorganisms in flow displacement systems, a distinction should be made between transparent substrata and nontransparent substrata. Phase-contrast microscopy is ideal for transparent substrata, but unfortunately dental enamel, bone, and metals, often being substrata for microbial adhesion in clinical microbiology, are not or not ideally transparent. It is a matter of choice whether one wants to change to transparent substrata in these cases. Although often microbial adhesion will be affected less by a

different choice of substratum after a proteinaceous conditioning film has developed as in most clinical conditions (33), microbial detachment may be strongly influenced by a different substratum choice and if possible one should preferably use the relevant material. For dental enamel, for instance, this can be achieved by preparing ultrathin enamel slides, with a thickness of around 30 µm. Such ultrathin enamel samples are essentially transparent when fixed on a glass slide and can be used in combination with phase-contrast microcopy (93).

Alternatively, if the sample possesses a certain reflectivity, incandescent dark-field illumination can be directed under a low angle of incidence, applying the light scattered by the adhering organisms for image formation (84). For metals, a metallurgical microscope, with incident light and applying the reflected light for imaging (94), gives surprisingly good images of adhering microorganisms.

The final solution of all imaging problems is based on the use of fluorescence microscopy, including the confocal laser scanning microscope. The additional advantage of this is that more advanced stages of biofilm formation, i.e., beyond the level of initial adhesion, can also be observed by optical sectioning techniques. Unfortunately, cell surface properties are often affected by staining or labeling (26) with a potential impact on their adhesion to substratum surfaces. *Escherichia coli* and *Serratia marcescens* strains, for instance, became slightly less hydrophobic, although not statistically significantly, upon green fluorescent labeling, depending on the *E. coli* strain involved. Caution should thus be practiced when performing adhesion experiments with labeled cells. Use of green fluorescent protein (GFP)-expressing cells circumvents these problems. GFP is fused to a constitutively expressed promoter, which ensures expression of the protein at any time during growth and development. Rice et al. (76) used GFP-expressing *Pseudomonas aeruginosa* to study biofilm formation in a parallel flow chamber in combination with confocal laser scanning microscopy. An additional advantage of the use of GFP promoter fusions is that it allows in situ visualization of gene expression (41).

The ultimate aim of the image analysis is to prepare a file with the number of adhering organisms as a function of time, preferably with adhering organisms separated according to single adhering organisms or higher-order multiplets. The first step in the analysis of the images obtained is discrimination of adhering organisms from the background and subsequently distinguishing between singly adhering organisms and multiplets. The human eye is superior to this end, but manual enumeration of adhering microorganisms on a surface is extremely time-consuming. Furthermore, it is often not realized that manual enumeration is not without error either. Meinders et al. (58) requested 19 experienced researchers to count several different types of bacteria adhering to a variety of substrata and reported a 5% standard deviation over the group.

During image collection, due to the finite depth of focus of all imaging systems, not only adhering organisms are captured, but also in-focus organisms moving along with the flow, just above the substratum surface. Clearly, these organisms must be eliminated from the enumeration (Fig. 10). This can be done by addition or multiplication of two subsequently stored images. Since moving organisms will appear at different locations in two subsequent images, the contrast of an adhering
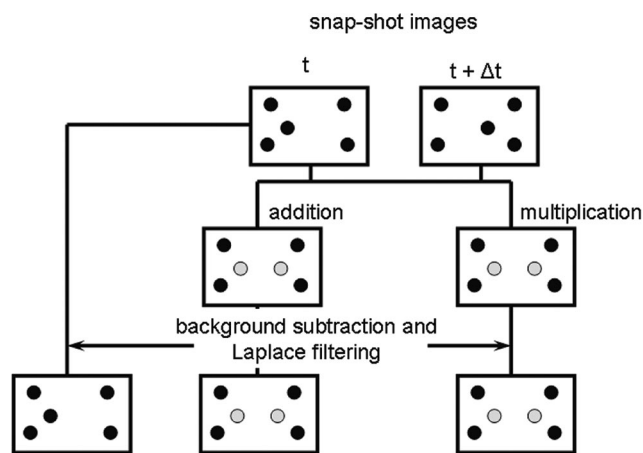

FIG. 10. Flow diagram of methods compared to eliminate in-focus flowing bacteria from automated image analysis. Top: Two snap-shot images taken at times t and $t + \Delta t$, with both adhering and flowing bacteria indicated in black. Left: Subtraction of both snap-shot images taken at t and $t + \Delta t$, and including background subtraction and Laplace filtering yields an image with only adhering bacteria (black dots). Middle and right: After addition (middle) or multiplication (right) of two snap-shot images, the background is subtracted and the image is Laplace filtered. As a result of this procedure the flowing bacteria obtain higher gray values than adhering bacteria. After filtration, the images are thresholded and the number of adhering bacteria can be determined.

organism will be enhanced this way. Next, a proper threshold has to be installed (58, 83), differentiating the gray value of an adhering organism from the background. Usually these steps suffice for reliable enumeration of adhering organisms with errors arising that are numerically similar to manual counting. Meinders et al. (58) even noted that addition or multiplication methods were strictly not necessary, provided the proper threshold was installed. Since, however, most researchers have difficulty installing the proper threshold, addition or multiplication methods are strongly recommended.

The next problem faced in automated enumeration is to determine the number of adhering organisms in adhering multiplets. Simple methods are based on area considerations, whereas the difficulty in solving this problem greatly depends on the resolution of the image analysis system. Wit and Busscher (106) proposed the use of an artificial neural network to teach the computer about shape, size, and contrast for determining what is an adhering organism. Artificial neural networks appeared highly useful for the enumeration of adhering organisms on subideal substrata such as slightly turbid silicone rubber. In other ways, artificial neural networks performed as well as conventional filters.

An extremely advanced mode of image analysis has been applied by Meinders et al. (57) to prepare a file containing not only the number of adhering organisms at each point in time, but also the times of arrival and departure of each adhering organism, in case of desorption. This method requires exact matching of different images, as a minor displacement of the field of view causes the analysis to decide that all adhering organisms have desorbed. Exact matching of images can be established, e.g., by particle tracking methods, as proposed later by Wit and Busscher (105).

Strategies for Data Analysis

Strategies for data analysis are numerous and the depth of analysis one wants to achieve, together with the sort of data file obtained, determines the final choice. We will describe strategies for data analysis, starting with the simplest possibility and ending with the most extensive one.

Strategy I. Presentation of the number of adhering bacteria per unit area at a fixed point in time is the simplest strategy, but in nearly all cases inadequate. Kinetic effects (see for instance Fig. 1) are completely neglected and erroneous conclusions regarding the ability of a given strain to adhere to a given substratum for its adhesiveness can easily result.

Strategy II. If a short time series, say of about 30 min, is obtained, this usually suffices to calculate the so-called initial deposition rate (j_0, cm^{-2} s^{-1}) from linear regression analysis of the number of adhering organisms versus time. Since the initial deposition rate reflects the interaction of an organism for a given substratum without intervening influences of already adhering organisms, this is a highly useful parameter, especially since it can be compared with the theoretical maximum for the experimental conditions applied according to Smoluchowski-Levich.

Strategy III. If the time series is more prolonged, it is recommended to calculate the initial deposition rate according to the above strategy (II) and subsequently evaluate adhesion in a more advanced state by presenting the number of organisms adhering in a more advanced state, i.e., after several hours (this then also reflects interactions between adhering organisms, apart from substratum interactions with the adhering organisms). Sometimes the data follow an exponential according to the following equation.

$$n(t) = n_\infty(1 - e^{-t/\tau}) \tag{6}$$

The characteristic adhesion time τ is determined by a combination of deposition, blocking and desorption, according to

$$1/\tau = \beta + j_0 A_b \tag{7}$$

in which A_b represents the area on the substratum surface blocked by one adhering bacterium and β is the desorption rate coefficient. One should be cautious, however, as frequently the above exponential function is poorly obeyed by adhering microorganisms.

Strategy IV. The two unknowns, A_b and β, from equation 7 can be further elaborated from blocked areas derived from so-called radial pair distribution functions $g(r)$, as can be calculated from the spatial arrangement of the adhering bacteria (Fig. 3). Radial pair distribution functions denote the local, relative density of adhering organisms as a function of the distance from a center organism, normalized with respect to the average density over the entire substratum. When microorganisms are randomly distributed over an entire substratum surface, $g(r)$ equals 1. However, if there is preferential adhesion at a given separation distance r between adhering bacteria, then $g(r)$ is >1. Figure 3 gives an example of a radial distribution function and as can be seen there is a certain distance from an adhering particle where the local density of adhering organisms is relatively low. This region can be associated with the blocked area A_b in equation 7, and therewith for the calculation of the desorption rate coefficient β.

TABLE 4. SLS-stimulated detachment of initially adhering *S. mutans* HG 985, early and late stage, in growing *S. mutans* biofilms from enamel surfaces in a parallel plate flow chamber

Biofilm type	Mean no. of bacteria on the surface before SLS[a] $\pm$ SD	Detachment (%)
Initial adhesion (2 h adhesion)	6.21 $\pm$ 1.78[b]	65
Early stage (4 h growth)	0.30 $\pm$ 0.14[c]	27
Late stage (16 h growth)	0.85 $\pm$ 0.16[c]	0

[a] Mean value over 10 images from random positions on the enamel surface. Data are from Landa et al. (43).
[b] Numbers of bacteria (10^6 cm^{-2}) from which the percent detachment is derived for initial adhesion.
[c] Fractional surface coverage from which the percent detachment is derived for early- and late-stage biofilms.

Strategy V. Finally, if residence times t_d to t_a have been successfully obtained, a time-dependent desorption rate coefficient (19) can be calculated that allows us to account for strengthening of the adhesive bond, as due for instance to extracellular polymeric substance (EPS) production by adhering organisms or other physicochemical processes occurring, such as the progressive removal of interfacial water. The time-dependent desorption rate coefficient is defined as

$$\beta(t - \tau) = \beta_\infty - (\beta_\infty - \beta_0)e^{-\delta[t - (t_d - t_a)]} \tag{8}$$

where $1/\delta$ is a characteristic time constant for bond aging. Depending on whether the initial desorption rate coefficient β_0 is larger or smaller than the final value β_∞, bonds are assumed to strengthen or weaken during aging. Combination of equation 8 with equations 6 and 7 yields, after some modification, complicated expressions for the number of adhering organisms as a function of time that are considered outside the scope of this review.

SELECTED EXAMPLES OF USE OF FLOW DISPLACEMENT SYSTEMS

Adhesion, Growth, and Detachment of *Streptococcus mutans* from Dental Enamel

S. mutans is considered one of the most cariogenic strains in the human oral cavity and preventive measures in dentistry are aimed at reducing its prevalence at the tooth surface. Application of detergents in oral health care products may assist dental plaque control through detachment of plaque organisms, although in most formulations detergents are added with the sole aim of stimulating foam formation, which is considered emotionally desirable by the consumer population (69). Sodium lauryl sulfate (SLS) is one detergent used to this end. When *S. mutans* was allowed to adhere to ultrathin dental enamel slabs (43), as described above, 6.2×10^6 bacteria could be adhered per cm^2 in 4 h and their detachment as induced by 4% (wt/vol) SLS solution was quite high (65%) (Table 4). However, if the flow chamber was perfused with defined medium supplemented with 0.2% glucose (43) medium after initial adhesion and adhering bacteria were allowed to grow, adhesion became much stronger, although image analysis did

TABLE 5. Initial deposition rates of *Candida* spp. to silicone rubber in the presence of adhering bacteria from either buffer or saliva, expressed as a percentage of the initial deposition rate of the yeast on silicone rubber in the absence of adhering bacteria[a]

Bacterial strain	Deposition rate (% of initial rate)					
	C. albicans GB 2/1		*C. krusei* GBJ 18/4a		*C. tropicalis* GB 9/9	
	Buffer	Saliva	Buffer	Saliva	Buffer	Saliva
R. dentocariosa GB 52b	3	**158**	3	59	26	98
R. dentocariosa GB 53d	3	**159**	6	51	47	87
S. aureus GB 2/1	8	**141**	4	94	35	**135**
S. epidermidis GB 9/6	9	10	5	26	23	60
S. epidermidis A GB 51b	4	29	6	44	23	70

[a] Results in excess of 100% are printed in bold. Results from triplicate experiments using freshly cultured bacteria and yeasts yield an average standard deviation of 30%. Data are from Millsap et al. (62).

not allow calculation of the number of adhering bacteria anymore and results had to be expressed in percent surface coverage. Based on the surface coverage, only 27% of the early biofilm could now be detached by SLS, whereas a late-stage biofilm was essentially irreversible.

Whereas the relevance of this study for dentistry has been described elsewhere (44), this experiment in the parallel plate flow chamber also shows the power of flow displacement systems to study bacterial adhesion and detachment in one and the same experiment. Moreover, at the same time, it illustrates the difference between initially adhering bacteria and bacteria adhering in a later stage of biofilm formation.

Growth of a *Pseudomonas aeruginosa* Biofilm in a Flow Displacement System

Biofilms are complex communities of microorganisms in the natural environment. The current conceptual model of a biofilm is an ingeniously complicated multispecies entity where ecological microniches are created and occupied by specific organisms (16). After attachment of the colonizing bacteria, growth of the sessile population occurs. Although there is a reasonable amount of research done on all the steps in biofilm formation (66), a great deal of current interest resides in understanding the manner in which reversibly adhered bacteria make the transition to irreversible adhesion. Using GFP-labeled *P. aeruginosa* (76), the growth characteristics of planktonic bacteria and the initially adhering and secondary biofilm bacteria have been compared in a parallel plate flow chamber. The initially adhering bacteria showed an increase of 15% in surface population during the first 12 h, whereas the secondary cells demonstrated an increase of surface population of 108% during 12 h. Planktonic bacteria did not have a lag time and showed an increase of 1,000% in population during the first 12 h. The results indicate that when a *P. aeruginosa* cell makes the transition from a planktonic to a sessile environment, there is a lag in growth. This observation is consistent with the concept that these cells undergo a phenotypic change. The amount of time to initiate these changes is very different and dependent on the

strain, solid substratum, and number of genes which are up- or downregulated (17).

Coadhesion of Yeast and Bacteria to Voice Prosthesis Material

Oropharyngeal infections due to adhering yeast and bacteria are common in AIDS patients (15) and bone marrow transplant recipients (37), while they are also responsible for a number of biomaterial-related infections, such as denture stomatitis (75) or malfunctioning of silicone rubber voice prostheses in laryngectomized patients (50, 67). A variety of different causative organisms have been identified, including *Candida* species, staphylococci, streptococci, and enterococci. *Candida* species have been associated with biomaterial ingrowth and deterioration of voice prostheses in general.

Adhesive interactions between yeast and bacteria on silicone rubber can also be determined in a parallel plate flow chamber (62) by preadhering bacteria on eight different positions on the bottom plate of a parallel plate flow chamber and subsequently measuring the deposition of yeast from a flowing suspension. Using this so-called dot assay, it has been observed that preadhesion of bacteria to a surface generally does not stimulate adhesion of yeasts (Table 5). Instead, it appeared that different bacterial strains suppressed adhesion of yeast to various degrees. Table 5 provides a selection of coadhesion data from Millsap et al. (61). In saliva, *Rothia dentocariosa* and *Staphylococcus aureus* GB 2/1 enhanced adhesion of yeasts, especially *Candida albicans*. This study shows that bacterial adhesion mostly reduces subsequent adhesion of yeasts, while only a few bacterial strains stimulate adhesion of yeasts, provided salivary adhesion mediators are present. Interestingly, different clinical studies have identified *Rothia dentocariosa* and *Staphylococcus aureus* in biofilms on explanted voice prostheses of patients needing extremely frequent replacement, while *C. albicans* is one of the yeasts generally held responsible for silicone rubber deterioration.

Flow displacement systems can thus also be ideally used to study adhesive interactions between microorganisms, while the time-consuming nature of the experiments has been circumvented in the dot assay as proposed by Millsap et al. (62) by preadhering eight different bacterial strains on different positions on a single bottom plate of the chamber.

TABLE 6. Initial deposition and detachment of *P. aeruginosa* strain 3 to Etafilcon A contact lenses in a parallel plate flow chamber prior to and after exposure of the lenses to four multipurpose lens care solutions[a]

Solution	j_0 (cm^{-2} s^{-1})	n_{2h} (10^6 cm^{-2})	d_{air} (%)	$d_{solution}$ (%)
Saline	1,617	10.7	1	0
Lens care (solution)				
A	1,259	8.9	9	15
B	2,221	9.4	0	35
C	3,138	12.0	5	32
D	1,842	8.0	6	42

[a] Data include initial deposition rates j_0, number of bacteria adhering after 2 h (n_{2h}), and percent detachment stimulated by the passage of an air bubble through the flow chamber (d_{air}) or by perfusing the chamber with a lens care solution ($d_{solution}$). Data are from Bruinsma et al. (11).

TABLE 7. Initial deposition rate, j_0, and number of adhering bacteria after 4 h on silicone rubber for *E. faecalis* 1131[a]

Drug	MIC	Initial deposition rate (j_0) (cm^{-2} s^{-1})	No. after 4 h (10^6 cm^{-2})
Ampicillin	0	226	2.2
	1/8	182	2.1
	1/4	94	1.5
Vancomycin	0	226	2.2
	1/8	552	4.8
	1/4	225	2.6

[a] The bacteria were grown in the presence and absence of ampicillin or vancomycin. Data are from Gallardo-Moreno et al. (27).

Adhesion of Bacteria to Contact Lenses and Interference by Lens Solutions

The number of people wearing contact lenses as an alternative to spectacles is steadily increasing and the use of contact lenses has become a major predisposing factor for the occurrence of microbially induced keratitis (48). Adhesion to and detachment of bacteria from contact lenses plays an important role in the development of infectious keratitis, where biofilms formed in contact lens casings provide a continuous source of microorganisms (32, 54). Cleansing of contact lens surfaces is facilitated through the use of lens care solutions to remove adsorbed tear film components and to kill and detach possible adhering bacteria (20).

Due to their finite dimensions, it is possible to fix contact lenses on the bottom plate of a parallel plate flow chamber and study bacterial adhesion and detachment by lens care solutions. Table 6 illustrates this possibility of flow displacement systems, summarizing the initial deposition rates of *Pseudomonas aeruginosa* 3 to Etafilcon A contact lenses after exposure to different lens care solutions, as well as the percent detachment of adhering bacteria by the passage of an air bubble or by perfusing the flow chamber with a lens care solution or physiological saline. Lens care solutions appeared to have different abilities to detach bacteria from contact lens surfaces, while all lens solutions involved in this study leave adsorbed components on contact lens surfaces, which positively or negatively influence adhesion of *P. aeruginosa* strain 3. Compared to a detergent such as sodium lauryl sulfate (43), however, these lens care solutions have very poor cleaning power and are aimed solely at killing the adhering bacteria, as evidenced by the low detachment percentages, which is unfortunate, as they leave a film of dead bacteria that acts as a substratum to which new bacteria can adhere (5).

Influence of Antibiotics on Bacterial Adhesion

Biomaterial-related infections are quite common (recent estimates by the Centers for Disease Control link 65% of all systemic infections to biofilm formation) and pose an enormous burden to the health care system, as the fate of an infected implant is usually removal. The path of entry of infecting organisms in this case can be perioperative, during hospitalization, or postoperative. Especially during perioperative infection and infection during hospitalization, adhering bacteria are likely to have been exposed to (sub)inhibitory concentrations of antibiotics. The exposure of bacteria to an-

tibiotics can reduce their adhesion to surfaces, as demonstrated by the reduction in *Staphylococcus epidermidis* adhesion to antibiotic-impregnated catheters (39), which has been associated with induction of biofilm-related gene expression in the same organism. However, adhesion of *Enterococcus faecalis* 1131 grown in the presence of one-eighth the MIC of vancomycin to silicone rubber in a parallel plate flow chamber (Table 7) demonstrated that a subinhibitory concentration of vancomycin increased adhesion of *Enterococcus faecalis* to silicone rubber (27), possibly as a survival mechanism to protect themselves on the surface against antibiotic attack. Ampicillin did not have such an effect.

This example of the use of the parallel plate flow chamber bears close relation to clinical practice, as the increased adhesion of the strain exposed to subinhibitory concentrations of vancomycin yields an important consideration before adding vancomycin to slow-release delivery systems (21, 34, 104), particularly because for many infectious strains, vancomycin is the drug of last resort and incorporation of other types of antibiotics (21, 52, 89, 99) has failed.

CONCLUSIONS

In conclusion, this review shows the potential of flow displacement systems in the study of microbial adhesion and detachment. Experimental set-up and ways to analyze data have been presented that will allow better comparison, on a more quantitative basis, of adhesion data from different laboratories over the world. Such is imperative to advance the field.

REFERENCES

1. **Alexandrou, A.** 2001. Combined analytic and experimental solutions, p. 266–343. *In* L. Curless, V. O'Brien, and D. A. George (ed.), Principles of fluid mechanics. Prentice Hall, Upper Saddle River, N.J.
2. **An, Y. H., and R. J. Friedman.** 1997. Laboratory methods for studies of bacterial adhesion. J. Microbiol. Methods **30:**141–152.
3. **Bakker, D. P., J. W. Klijnstra, H. J. Busscher, and H. C. van der Mei.** 2003. The effect of dissolved organic carbon on bacterial adhesion to conditioning films adsorbed on glass from natural seawater collected during different seasons. Biofouling **19:**391–397.
4. **Bakker, D. P., A. van der Plaats, G. J. Verkerke, H. J. Busscher, and H. C. van der Mei.** 2003. A comparison of velocity profiles in different flow chamber designs used in studies of microbial adhesion to surfaces. Appl. Environ. Microbiol. **69:**6280–6287.
5. **Banks, M. K., and J. D. Bryers.** 1992. Deposition of bacterial cells onto glass and biofilm surfaces. Biofouling **6:**81–86.
6. **Bos, R., H. C. van der Mei, and H. J. Busscher.** 1999. Physico-chemistry of initial microbial adhesive interactions—its mechanisms and methods for study. FEMS Microbiol. Rev. **23:**179–230.
7. **Bos, R., H. C. van der Mei, J. Gold, and H. J. Busscher.** 2000. Retention of bacteria on a substratum surface with micro-patterned hydrophobicity. FEMS Microbiol. Lett. **189:**311–315.
8. **Bourne, M. C.** 2002. Food texture and viscosity: concept and measurement, p. 14–31. Academic Press, San Diego, Calif.
9. **Bowen, B. D.** 1985. Streaming potential in the hydrodynamic entrance region of cylindrical and rectangular capillaries. J. Colloid Interface Sci. **106:**367–376.
10. **Bretherton, F. P.** 1961. The motion of long bubbles in tubes. J. Fluid Mech. **10:**166–188.
11. **Bruinsma, G. M., J. de Vries, H. C. van der Mei, and H. J. Busscher.** 2001. Adhesion of *Pseudomonas aeruginosa* to contact lenses after exposure to multi-purpose lens care solutions. J. Adhesion Sci. Technol. **15:**1453–1462.
12. **Busscher, H. J., G. I. Geertsema-Doornbusch, and H. C. van der Mei.** 1997. Adhesion to silicone rubber of yeasts and bacteria isolated from voice prostheses: influence of salivary conditioning films. J. Biomed. Mat. Res. **34:**201–210.
13. **Chang, H. T., B. E. Rittman, D. Amar, R. Heim, O. Ehrlinger, and Y. Lesty.** 1991. Biofilm detachment mechanisms in a liquid-fluidized bed. Biotechnol. Bioeng. **38:**499–506.
14. **Christersson, C. E., P.-O. Glantz, and R. E. Baier.** 1988. Role of temper-

ature and shear force on microbial detachment. Scand. J. Dent. Res. **96:**91–98.

15. **Coleman, D. C., D. E. Bennett, D. J. Sullivan, P. J. Gallagher, M. C. Henman, D. B. Shanley, and R. J. Russell.** 1993. Oral *Candida* in HIV infection in AIDS: new perspectives/new approaches. Crit. Rev. Microbiol. **19:**61–82.

16. **Costerton, J. W.** 1995. Overview of microbial biofilms. J. Ind. Microbiol. **15:**137–140.

17. **Costerton, J. W., Z. Lewandowski, D. E. Caldwell, D. R. Korber, and H. M. Lappin-Scott.** 1995. Microbial biofilms. Annu. Rev. Microbiol. **49:**711–745.

18. **Cutter, L. A., P. M. van Schie, and M. Fletcher.** 2003. Adhesion of anaerobic microorganisms to solid surfaces and the effect of sequential attachment on adhesion characteristics. Biofouling **19:**9–18.

19. **Dabros, T., and T. G. M. van de Ven.** 1982. Kinetics of coating by colloidal particles. J. Colloid Interface Sci. **89:**232–244.

20. **Dannelly, H. K., and R. V. M. S. Waworuntu.** 2004. Effectiveness of contact lens disinfectants after lens storage. Eye Contact Lens **30:**163–165.

21. **Dash, A. K., and G. C. Cudworth.** 1998. Therapeutic applications of implantable drug delivery systems. J. Pharmacol. Toxicol. Methods **40:**1–12.

22. **Elimelech, M.** 1994. Particle deposition on ideal collectors from dilute flowing suspensions: mathematical formulation, numerical solution, and simulations. Sep. Technol. **4:**186–212.

23. **Fang, H. H. P., K.-Y. Chan, and L.-C. Xu.** 2000. Quantification of bacterial adhesion forces using atomic force microscopy (AFM). J. Microbiol. Methods **40:**89–97.

24. **Fielden, M., R. A. Hayes, and J. Ralston.** 1996. Surface and capillary forces affecting air bubble-particle interactions in aqueous electrolytes. Langmuir **12:**3721–3727.

25. **Flemming, H. C., and J. Wingender.** 2000. Relevance of microbial polymeric substances (EPSs). I. Structural and ecological aspects. Water Sci. Technol. **43:**1–8.

26. **Fuller, M. E., S. H. Streger, R. K. Rothmel, B. J. Mailloux, J. A. Hall, T. C. Onstott, J. K. Fredrickson, D. L. Balkwill, and M. F. DeFlaun.** 2000. Development of a vital fluorescent staining method for monitoring bacterial transport in subsurface environments. Appl. Environ. Microbiol. **66:**4486–4496.

27. **Gallardo-Moreno, A. M., H. C. van der Mei, H. J. Busscher, M. L. Gonzalez-Martin, J. M. Bruque, and C. Perez-Giraldo.** 2001. Adhesion of *Enterococcus faecalis* 1131 grown under subinhibitory concentrations of ampicillin and vancomycin to a hydrophilic and a hydrophobic substratum. FEMS Microbiol. Lett. **203:**75–79.

28. **Gelhard, T. B., V. Fidler, E. J. s-Gravenmade, and A. Vissink.** 1983. Remineralization of softened human enamel in mucin- or CMC-containing artificial salivas. J. Oral Pathol. **12:**336–341.

29. **George, R. P., P. Mulareedharan, K. R. Sreekumari, and H. S. Khatak.** 2003. Influence of surface characteristics and microstructure on adhesion of bacterial cells onto a type 304 stainless steel. Biofouling **19:**1–8.

30. **Gómez-Suárez, C., H. J. Busscher, and H. C. van der Mei.** 2001. Analysis of bacterial detachment from substratum surfaces by the passage of air-liquid interfaces. Appl. Environ. Microbiol. **67:**2531–2537.

31. **Gómez-Suárez, C., H. C. van der Mei, and H. J. Busscher.** 2002. Adhesion, immobilization, and retention of microorganisms on solid substrata, p. 100–113. *In* G. Bitton (ed.), Encyclopedia of environmental microbiology. John Wiley and Sons, Inc., New York, N.Y.

32. **Gray, T. B., R. T. Cursons, J. F. Sherwan, and P. R. Rose.** 1995. Acanthamoeba, bacterial, and fungal contamination of contact lens storage cases. Br. J. Ophthalmol. **79:**601–605.

33. **Gristina, A. G.** 1987. Biomaterials-centered infection: microbial adhesion versus tissue integration. Science **237:**1588–1597.

34. **Gursel, I., F. Korkusuz, F. Turesin, N. G. Alaeddinoglu, and V. Hasirci.** 2001. In vivo application of biodegradable controlled antibiotic release systems for the treatment of implant-related osteomyelitis. Biomaterials **22:**73–80.

35. **Hewitt, D., D. Fornasiero, and J. Ralston.** 1995. Bubble-particle attachment. J. Chem. Soc. Faraday Trans. **94:**1997–2001.

36. **Hewitt, D., D. Fornasiero, J. Ralston, and L. R. Fisher.** 1998. Aqueous film drainage at the quartz/water/air interface. J. Chem. Soc. Faraday Trans. **89:**817–822.

37. **Hsu, L. Y., G. E. Minah, D. E. Peterson, J. R. Wingard, W. G. Merz, V. Altomonte, and C. A. Tylenda.** 1990. Coaggregation of oral *Candida* isolates with bacteria from bone marrow transplant recipients. J. Clin. Microbiol. **28:**2621–2626.

38. **Hung, G., F. Hsu, and L. Stark.** 1977. Dynamics of the human eyeblink. Am. J. Optom. Physiol. Opt. **54:**678–690.

39. **Kohnen, W., C. Kolbenschlag, S. Teske-Keiser, and B. Jansen.** 2003. Development of a long-lasting ventricular catheter impregnated with a combination of antibiotics. Biomaterials **24:**4865–4869.

40. **Korber, D. R., J. R. Lawrence, L. Zhang, and D. E. Caldwell.** 1990. Effect of gravity on bacterial deposition and orientation in laminar flow environments. Biofouling **2:**335–350.

41. **Korber, D. R., G. M. Wolfaardt, V. Brozel, R. MacDonald, and T. Niepel.**

42. **Krumbein, W. E.** 1996. Geophysiology and parahistology of the interactions of organisms with the environment. Mar. Ecol. **17:**1–23.

43. **Landa, A. S., B. van de Belt-Gritter, H. C. van der Mei, and H. J. Busscher.** 1999. Recalcitrance of *Streptococcus mutans* biofilms towards detergent-stimulated detachment. Eur. J. Oral Sci. **107:**236–243.

44. **Landa, A. S., H. C. van der Mei, and H. J. Busscher.** 1997. Detachment of linking film bacteria from enamel surfaces by oral rinses and penetration of sodium laurylsulphate through an artificial oral biofilm. Adv. Dent. Res. **11:**528–538.

45. **Landa, A. S., H. C. van der Mei, and H. J. Busscher.** 1996. A comparison of the detachment of an adhering oral streptococcal strain stimulated by mouthrinses and a pre-brushing rinse. Biofouling **9:**327–339.

46. **Leach, S. A., K. J. Swindin, and K. C. Shaw.** 1985. The restoration of fimbriae to laboratory grown streptococci by the oral environment, p. 63–74. *In* P. O. Glantz, S. A. Leach, and T. Ericson (ed.), Oral interfacial reactions of bone, soft tissue and saliva. IRL Press Ltd., Oxford, England.

47. **Leenaars, A. F. M., and S. B. G. O'Brien.** 1989. A new approach to the removal of sub-micron particles from solid (silicon) substrates, p. 361–372. *In* K. L. Mittal (ed.), Particles on surfaces: detection, adhesion and removal. Plenum Press, New York, N.Y.

48. **Liesegang, T. J.** 1997. Contact lens-related microbial keratitis. II. Pathophysiology. Cornea **16:**125–131.

49. **Liu, Y., and J. H. Tay.** 2002. The essential role of hydrodynamic shear forces in the formation of biofilm and granular sludge. Water Res. **36:**1653–1665.

50. **Mahieu, H. F., H. F. K. van Saene, H. J. Rosingh, and H. K. Schutte.** 1986. Candida vegetations on silicone voice prostheses. Arch. Otolaryngol. Head Neck Surg. **112:**321–325.

51. **Marshall, K. C.** 1985. Mechanisms of bacterial adhesion at solid-water interfaces, p. 133–161. *In* D. C. Savage and M. Fletcher (ed.), Bacterial adhesion. Plenum Press, New York, N.Y.

52. **Matsuda, K., S. Suzuki, N. Isshiki, K. Yoshioka, T. Okada, S. H. Hyon, and Y. Ikada.** 1991. A bilayer "artificial skin" capable of sustained release of an antibiotic. Br. J. Plast. Surg. **44:**142–146.

53. **McCabe, W. L., and J. C. Smith.** 1976. Fluid mechanics, p. 84–112. *In* S. D. Kirkpatrick (ed.), Unit operations of chemical engineering. McGraw-Hill, New York, N.Y.

54. **McLaughlin-Borlace, L., F. Stapleton, M. Matheson, and J. K. Dart.** 1998. Bacterial biofilm on contact lenses and lens storage cases in wearers with microbial keratitis. J. Appl. Microbiol. **85:**827–838.

55. **Medilanski, E., L. Y. Wick, O. Wanner, and H. Harms.** 2003. Mutual influences of *Pseudomonas aeruginosa* and *Desulfovibrio desulfuricans* on their adhesion to stainless steel. Biofouling **19:**125–132.

56. **Meinders, J. M., and H. J. Busscher.** 1994. Adsorption and desorption of colloidal particles on glass in a parallel plate flow chamber-influence of ionic strength and shear rate. Colloid Polymer Sci. **272:**478–486.

57. **Meinders, J. M., J. Noordmans, and H. J. Busscher.** 1992b. Simultaneous monitoring of the adsorption and desorption of colloidal particles during deposition in a parallel plate flow chamber. J. Colloid Interface Sci. **152:**265–280.

58. **Meinders, J. M., H. C. van der Mei, and H. J. Busscher.** 1992. In situ enumeration of bacterial adhesion in a parallel plate flow chamber—elimination of in focus flowing bacteria from the analysis. J. Microbiol. Methods **16:**119–124.

59. **Meinders, J. M., H. C. van der Mei, and H. J. Busscher.** 1994. Physicochemical aspects of deposition of *Streptococcus thermophilus* B to hydrophobic and hydrophilic substrata in a parallel plate flow chamber. J. Colloid Interface Sci. **164:**355–363.

60. **Meinders, J. M., H. C. van der Mei, and H. J. Busscher.** 1995. Deposition efficiency and reversibility of bacterial adhesion under flow. J. Colloid Interface Sci. **176:**329–341.

61. **Millsap, K. W., R. Bos, H. C. van der Mei, and H. J. Busscher.** 1999. Adhesion and surface-aggregation of *Candida albicans* from saliva on acrylic surfaces with adhering bacteria as studied in a parallel plate flow chamber. Antonie Leeuwenhoek **75:**351–359.

62. **Millsap, K. W., R. Bos, H. C. van der Mei, and H. J. Busscher.** 2000. Dot assay for determining adhesive interactions between yeasts and bacteria under controlled hydrodynamic conditions. J. Microbiol. Methods **40:**225–232.

63. **Ming, F., W. Whish, J. Hubble, and R. Eisenthal.** 1998. Estimation of parameters for cell-surface interactions: maximum binding force and detachment constant. Enzymol. Microbiol. Technol. **22:**94–99.

64. **Mohamed, N., T. R. Rainier, and J. M. Ross.** 2000. Novel experimental study of receptor-mediated bacterial adhesion under the influence of fluid shear. Biotechnol. Bioeng. **68:**628–636.

65. **Morisaki, H.** 1991. Measurement of the force necessary for removal of bacterial cells from a quartz plate. J. Gen. Microbiol. **137:**2649–2655.

66. **Mueller, R. F., W. G. Characklis, W. L. Jones, and J. T. Sears.** 1992. Characterization of initial events in bacterial surface colonization by two

1999. Reporter systems for microscopic analysis of microbial biofilms. Methods Enzymol. **310:**3–20.

Pseudomonas species using image analysis. Biotechnol. Bioeng. **39:**1161–1170.

67. **Neu, T. R., H. C. van der Mei, H. J. Busscher, F. Dijk, and G. J. Verkerke.** 1993. Biodeterioration of medical-grade silicone rubber used for voice prostheses: a SEM study. Biomaterials **14:**459–464.

68. **Nguyen-Van, A.** 1994. The collision of fine particles and single air-bubbles in flotation. J. Colloid Interface Sci. **162:**123–128.

69. **Pader, M.** 1985. Oral hygiene products, p. 293–348. *In* M. M. Rieger (ed.), Surfactants in cosmetics. Marcel Dekker, New York, N.Y.

70. **Palmer, J. R., and D. E. Caldwell.** 1995. A flow cell for the study of plaque removal and regrowth. J. Microbiol. Methods **24:**171–182.

71. **Palmer, J. R., S. M. Gordon, J. O. Cisar, and P. E. Kolenbrander.** 2003. Coaggregation-mediated interactions of streptococci and actinomyces detected in initial human dental plaque. J. Bacteriol. **185:**3400–3409.

72. **Pereira, M. O., M. Kuehn, S. Wuertz, T. Neu, and L. F. Melo.** 2002. Effect of flow regime on the architecture of a *Pseudomonas fluorescens* biofilm. Biotechnol. Bioeng. **78:**164–171.

73. **Pitt, W. G., M. O. McBride, A. J. Barton, and R. D. Sagers.** 1993. Air-water interfaces displace adsorbed bacteria. Biomaterials **14:**605–608.

74. **Prakobphol, A., C. A. Burdsal, and S. J. Fisher.** 1995. Quantifying the strength of bacterial adhesive interactions with salivary glycoproteins. J. Dent. Res. **74:**1212–1218.

75. **Radford, D. R., S. J. Challacombe, and J. D. Walter.** 1999. Denture plaque and adherence of *Candida albicans* to denture-base materials in vivo and in vitro. Crit. Rev. Oral Biol. Med. **10:**99–116.

76. **Rice, A. R., M. A. Hamilton, and A. K. Camper.** 2000. Apparent surface associated lag time in growth of primary biofilm cells. Microb. Ecol. **41:**8–15.

77. **Rickard, A. H., A. J. McBain, A. T. Stead, and P. Gilbert.** 2004. Shear rate moderates community diversity in fresh water biofilms. Appl. Environ. Microbiol. **70:**7426–7435.

78. **Rutter, P. R., and B. Vincent.** 1988. Attachment mechanisms in the surface growth of microorganisms, p. 87–107. *In* M. J. Bazin and J. I. Prosser (ed.), Physiological models in microbiology. CRC Press, Boca Raton, Fla.

79. **Saleh, S., J. F. Throvert, and P. M. Adler.** 1993. Flow along porous media by particle image velocimetry. AIChE J. **39:**1765–1776.

80. **Schneider, R. P.** 1996. Conditioning film-induced modification of substratum physicochemistry. Analysis by contact angles. J. Colloid Interface Sci. **182:**2004–2213.

81. **Schulze, H. J., B. Wahl, and G. Gottschalk.** 1989. Determination of adhesive strength of particles with the liquid/gas interface in flotation by means of a centrifugal method. J. Colloid Interface Sci. **128:**57–65.

82. **Sjollema, J., H. J. Busscher, and A. H. Weerkamp.** 1988. Deposition of oral streptococci and polystyrene lattices onto glass in a parallel plate flow cell. Biofouling **1:**101–112.

83. **Sjollema, J., H. J. Busscher, and A. H. Weerkamp.** 1989. Real time enumeration of adhering microorganisms in a parallel plate flow cell using automated image analysis. J. Microbiol. Methods **9:**73–78.

84. **Sjollema, J., H. J. Busscher, and A. H. Weerkamp.** 1989. Experimental approaches for studying adhesion of microorganisms to solid substrata: applications and mass transport. J. Microbiol. Methods **9:**79–90.

85. **Stoodley, P., R. Cargo, C. J. Rupp, S. Wilson, and I. Klapper.** 2002. Biofilm material properties as related to shear-induced deformation and detachment phenomena. J. Ind. Microbiol. Biotechnol. **29:**361–367.

86. **Stoodley, P., D. De Beer, and Z. Lewandowski.** 1994. Liquid flow in biofilm systems. Appl. Environ. Microbiol. **60:**2711–2716.

87. **Stoodley, P. L., L. Hall-Stoodley, and H. M. Lappin-Scott.** 2001. Detachment, surface migration and other dynamic behaviour in bacterial biofilms revealed by digital time-lapse imaging. Methods Enzymol. **337:**306–319.

88. **Tanner, J., A. Carlen, E. Soderling, and P. K. Vallitu.** 2003. Adsorption of parotid saliva proteins and adhesion of *Streptococcus mutans* ATCC 21752 to dental fiber-reinforced composites. J. Biomed. Mat. Res. B **66B:**391–398.

89. **Ueng, S. W., S. S. Lee, S. S. Lin, E. C. Chan, B. R. Hsu, and K. T. Chen.** 2000. Biodegradable alginate antibiotic beads. Clin. Orthop. **380:**250–259.

90. **Vadillo-Rodriguez, V., H. J. Busscher, W. Norde, J. de Vries, and H. C. van der Mei.** 2004. Atomic force microscopic corroboration of bond-aging for adhesion of *Streptococcus thermophilus* to solid substrata. J. Colloid Interface Sci. **278:**251–254.

91. **van der Mei, H. C., P. Brokke, J. Dankert, J. Feijen, and H. J. Busscher.** 1992. Influence of electrostatic interactions on the deposition efficiencies of coagulase-negative staphylococci to collector surfaces in a parallel plate flow chamber. J. Disp. Sci. Technol. Spec. Iss. Biocolloids Biosurfaces **13:**447–458.

92. **van der Mei, H. C., J. M. Meinders, and H. J. Busscher.** 1994. The influence of ionic strength and pH on diffusion of microorganisms with different structural surface features. Microbiology **140:**3113–3419.

93. **van der Mei, H. C., D. J. White, E. R. Cox, G. I. Geertsema-Doornbusch, and H. J. Busscher.** 2002. Bacterial detachment from salivary conditioning films by dentifrice supernates. J. Clin. Dent. **13:**44–49.

94. **Van Hoogmoed, C. G., H. C. van der Mei, and H. J. Busscher.** 1997. The influence of calcium on the initial adhesion of *S. thermophilus* to stainless steel under flow studied by metallurgical microscopy. Biofouling **11:**167–176.

95. **Van Loosdrecht, M. C. M., J. Lyklema, W. Norde, and A. B. Zehnder.** 1989. Bacterial adhesion: a physicochemical approach. Microb. Ecol. **17:**1–15.

96. **Van Wagenen, R. J., and J. D. Andrade.** 1980. Flat plate streaming potential investigations: hydrodynamics and electrokinetic equivalency. J. Colloid Interface Sci. **76:**305–314.

97. **Vassilakos, N., S. Kalfas, T. Arnebrant, and J. Rundegren.** 1993. A simple flow cell system to evaluate in vitro bacterial adhesion on solids. Colloids Surf. B **1:**341–347.

98. **Velraeds, M. M. C., H. C. van der Mei, G. Reid, and H. J. Busscher.** 1997. Inhibition of initial adhesion of uropathogenic *Enterococcus faecalis* to solid substrata by an adsorbed biosurfactant layer from *Lactobacillus acidophilus*. Urology **49:**790–794.

99. **Veyries, M. L., G. Couarraze, S. Geiger, F. Agnely, L. Massias, B. Kunzli, F. Faurisson, and B. Rouveix.** 1999. Controlled release of vancomycin from poloxamer 407 gels. Int. J. Pharm. **192:**183–193.

100. **Vieira, M. J., L. F. Melo, and M. M. Pinheiro.** 1993. Biofilm formation: hydrodynamic effects on internal diffusion and structure. Biofouling **7:**67–80.

101. **Waar, K., H. C. van der Mei, H. J. M. Harmsen, J. E. Degener, and H. J. Busscher.** 2002. Adhesion to bile drain materials and physicochemical surface properties of *Enterococcus faecalis* strains grown in the presence of bile. Appl. Environ. Microbiol. **68:**3855–3858.

102. **Wijeyekoon, S., T. Mino, H. Satoh, and T. Matsuo.** 2000. Growth and novel structural features of tubular biofilms produced under different hydrodynamic conditions. Water Sci. Technol. **41:**129–138.

103. **Wimpenny, J. W. T., and R. Colasanti.** 1997. A unifying hypothesis for the structure of microbial biofilms based on cellular automaton models. FEMS Microbiol. Ecol. **22:**1–16.

104. **Winkler, H., O. Janata, C. Berger, W. Wein, and A. Georgopoulos.** 2000. In vitro release of vancomycin and tobramycin from impregnated human and bovine bone grafts. J. Antimicrob. Chemother. **46:**423–428.

105. **Wit, P. J., and H. J. Busscher.** 1995. Tracking of colloidal particles using microscopic image sequence analysis. Colloids Surf. A **125:**85–92.

106. **Wit, P. J., and H. J. Busscher.** 1998. Application of an artificial neural network in the enumeration of yeasts and bacteria adhering to solid substrata. J. Microbiol. Methods **32:**281–290.

107. **Xia, Z., L. Woo, and T. G. M. van de Ven.** 1989. Microrheological aspects of adhesion of *Escherichia coli* on glass. Biorheology **26:**359–375.